NASA TECHNICAL NOTE

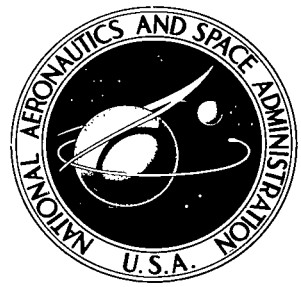

NASA TN D-6531

NASA TN D-6531

COMPARISON OF SEVERAL METHODS FOR ESTIMATING LOW-SPEED STABILITY DERIVATIVES FOR TWO AIRPLANE CONFIGURATIONS

by Herman S. Fletcher

Langley Research Center
Hampton, Va. 23365

NATIONAL AERONAUTICS AND SPACE ADMINISTRATION • WASHINGTON, D. C. • NOVEMBER 1971

ERRATA

NASA Technical Note D-6531

COMPARISON OF SEVERAL METHODS FOR ESTIMATING LOW-SPEED STABILITY DERIVATIVES FOR TWO AIRPLANE CONFIGURATIONS

By Herman S. Fletcher

November 1971

Page 10: Under the section entitled "C_{l_r} (fig. 17)," delete the last sentence: "The equation given in reference 4 for the tail contribution to C_{l_r} appears to have a sign error, which causes the C_{l_r} value to be too negative."

Then, reword the entire section as follows:

C_{l_r} (fig. 17).- Figure 17 shows that the estimated values of C_{l_r} were in fair agreement with each other for the unswept- and swept-wing configurations.

Page 33: Replace figure 17 with the attached corrected figure.

Issued October 1972

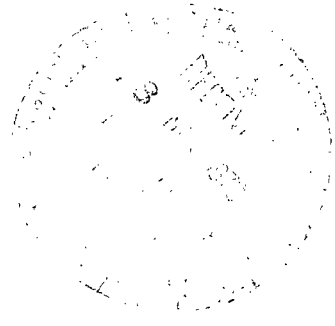

NASA-Langley, 1972

Errata inserted
10-Nov 72 JK

1. Report No.	2. Government Accession No.	3. Recipient's Catalog No.
NASA TN D-6531		

4. Title and Subtitle
COMPARISON OF SEVERAL METHODS FOR ESTIMATING LOW-SPEED STABILITY DERIVATIVES FOR TWO AIRPLANE CONFIGURATIONS

5. Report Date
November 1971

6. Performing Organization Code

7. Author(s)
Herman S. Fletcher

8. Performing Organization Report No.
L-7914

9. Performing Organization Name and Address
NASA Langley Research Center
Hampton, Va. 23365

10. Work Unit No.
136-62-02-04

11. Contract or Grant No.

12. Sponsoring Agency Name and Address
National Aeronautics and Space Administration
Washington, D.C. 20546

13. Type of Report and Period Covered
Technical Note

14. Sponsoring Agency Code

15. Supplementary Notes

16. Abstract

Methods presented in five different publications have been used to estimate the low-speed stability derivatives of two unpowered airplane configurations. One configuration had unswept lifting surfaces; the other configuration was the D-558-II swept-wing research airplane. The results of the computations were compared with each other, with existing wind-tunnel data, and with flight-test data for the D-558-II configuration to assess the relative merits of the methods for estimating derivatives. The results of the study indicated that, in general, for low subsonic speeds, no one text appeared consistently better for estimating all derivatives.

17. Key Words (Suggested by Author(s))
Calculated and experimental stability derivatives
Swept-wing and unswept-wing configurations
Low speeds

18. Distribution Statement
Unclassified – Unlimited

19. Security Classif. (of this report)	20. Security Classif. (of this page)	21. No. of Pages	22. Price*
Unclassified	Unclassified	33	$3.00

*For sale by the National Technical Information Service, Springfield, Virginia 22151

COMPARISON OF SEVERAL METHODS FOR ESTIMATING LOW-SPEED STABILITY DERIVATIVES FOR TWO AIRPLANE CONFIGURATIONS

By Herman S. Fletcher
Langley Research Center

SUMMARY

Methods presented in five different publications have been used to estimate the low-speed stability derivatives of two unpowered airplane configurations. One configuration had unswept lifting surfaces; the other configuration was the D-558-II swept-wing research airplane. The results of the computations were compared with each other, with existing wind-tunnel data, and with flight-test data for the D-558-II configuration to assess the relative merits of the methods for estimating derivatives.

In general, it was found that all the methods gave reasonably accurate predictions for those derivatives which are attributed primarily to the wing and horizontal tail – mainly, the longitudinal derivatives. Even in these instances, however, there was some variation in the estimated horizontal tail and fuselage contribution to the pitching moments.

There were large differences between some of the lateral derivatives computed by using the various estimation methods. Most of the differences can be traced to the estimated vertical-tail effectiveness. A detailed comparison of tail-effectiveness estimates is not feasible because of differences in definitions of effective areas, span, interference effects, and so on.

The results of this study indicate that, in general, for low subsonic speeds, no one text appeared consistently better for estimating all derivatives.

INTRODUCTION

Aerodynamic derivatives of airplanes are required for several types of analyses, such as stability calculations, motion response, and man-machine simulation. In order for the results of such analyses to be valid, it is necessary that the derivatives be accurate. There are three general methods of obtaining aerodynamic derivatives of a complete airplane, and these are

(1) Analytical methods based on theory and on empirical relations derived from accumulated wind-tunnel data

(2) Wind-tunnel tests of the airplane or a model of the airplane

(3) Analysis of flight data

Each of these basic methods is subject to some limitations and interpretations. There are several documents available in which techniques are presented for estimating derivatives (e.g., refs. 1 to 5). There are also several techniques available for extracting derivatives from flight data.

A recent publication (ref. 6) compared the stability derivatives of a Navion aircraft as determined by several textbook methods, from wind-tunnel tests, and from flight data. There were large differences in some of the more important derivatives. The reasons for the differences in some instances were not identified.

The present study was initiated to determine whether there are basic differences in the various published methods, to point out the differences found, and to assess the relative merits of the methods for estimating the low-speed stability derivatives. The study is based on computation by various methods of the derivatives for two specific airplane configurations for which much wind-tunnel data were available. Considerable flight data also were available for one of the configurations. In addition, some other comparisons are available for flight, wind-tunnel, and theoretical derivatives (for example, refs. 7 to 19). However, these references are different in scope and for other airplane configurations than those considered herein.

SYMBOLS

The calculated, experimental, and flight-extracted derivatives are presented in the form of standard NASA coefficients and moments about the stability axes. Values are given in both SI and U.S. Customary Units. The measurements and calculations were made in U.S. Customary Units. The coefficients and symbols used herein are defined as follows:

b span, meters (feet)

$\bar{c}$ mean aerodynamic chord, meters (feet)

q_V dynamic pressure at vertical tail, newtons per meter^2 (pounds per foot^2)

q_∞ free-stream dynamic pressure, newtons per meter^2 (pounds per foot^2)

S wing area, meters^2 (feet^2)

t	time, seconds
α	angle of attack of body reference line, radians
$\dot{\alpha} = d\alpha/dt$	
β	sideslip angle, $\sin^{-1}\frac{v}{V_\infty}$, radians
$d\epsilon/d\alpha$	change in downwash angle with angle of attack
$\partial\sigma/\partial\beta$	change in sidewash angle at tail with change in sideslip angle
M	Mach number
p	rolling velocity, radians per second
q	pitching velocity, radians per second
r	yawing velocity, radians per second
V_∞	free-stream velocity, meters per second (feet per second)
v	velocity along Y-axis, meters per second (feet per second)
$pb/2V_\infty$	wing-tip helix angle, radians
$rb/2V_\infty$	yawing-angular-velocity parameter, radians
F_L	lift, newtons (pounds)
F_Y	side force, newtons (pounds)
M_X	rolling moment, meter-newtons (foot-pounds)
M_Y	pitching moment about center of gravity, meter-newtons (foot-pounds)
M_Z	yawing moment, meter-newtons (foot-pounds)
C_L	lift coefficient, $F_L/q_\infty S$

C_l rolling-moment coefficient, $M_X/q_\infty Sb$

C_m pitching-moment coefficient, $M_Y/q_\infty S\bar{c}$

C_n yawing-moment coefficient, $M_Z/q_\infty Sb$

C_Y side-force coefficient, $F_Y/q_\infty S$

C_{L_α} lift-curve slope, $\partial C_L/\partial\alpha$, per radian

C_{m_α} pitching-moment-curve slope, $\partial C_m/\partial\alpha$, per radian

$C_{m_{\dot{\alpha}}}$ angle-of-attack damping parameter, $\partial C_m \Big/ \partial\frac{\dot{\alpha}\bar{c}}{2V_\infty}$, per radian

C_{l_β} rolling moment due to sideslip or effective-dihedral parameter, $\partial C_l/\partial\beta$, per radian

C_{n_β} yawing moment due to sideslip or directional-stability parameter, $\partial C_n/\partial\beta$, per radian

C_{Y_β} side force due to sideslip, $\partial C_Y/\partial\beta$, per radian

C_{m_q} damping-in-pitch parameter, $\partial C_m \Big/ \partial\frac{q\bar{c}}{2V_\infty}$, per radian

$C_{m_q}+C_{m_{\dot{\alpha}}}$ effective damping-in-pitch parameter, per radian

C_{l_p} rolling moment due to rolling velocity or damping-in-roll parameter, $\partial C_l \Big/ \partial\frac{pb}{2V_\infty}$, per radian

C_{n_p} yawing moment due to rolling velocity or adverse-yaw parameter, $\partial C_n \Big/ \partial\frac{pb}{2V_\infty}$, per radian

C_{Y_p} side force due to rolling velocity, $\partial C_Y \Big/ \partial\frac{pb}{2V_\infty}$, per radian

C_{l_r} rolling moment due to yawing velocity, $\partial C_l \Big/ \partial\frac{rb}{2V_\infty}$, per radian

C_{n_r} yawing moment due to yawing velocity or damping-in-yaw parameter, $\partial C_n \Big/ \partial\frac{rb}{2V_\infty}$, per radian

C_{Y_r} side force due to yawing velocity, $\partial C_Y / \partial \frac{rb}{2V_\infty}$, per radian

Subscript:

V vertical tail

Model component designations:

W wing

WF wing-fuselage

V vertical tail

H horizontal tail

WFVH complete model or airplane

AIRPLANE CONFIGURATIONS

The airplane configurations selected for this study are shown in figures 1 and 2. Figure 1 is a drawing of the general research model which was used in several wind-tunnel studies as part of a series of investigations to determine the effects of airplane geometry on stability derivatives. Figure 2 is a drawing of the D-558-II swept-wing airplane. Much wind-tunnel data from model tests and some flight data obtained with the full-scale airplanes are available for comparison with estimated derivatives. The two configurations vary appreciably from each other in geometric appearance, which is desirable for this type of analysis. Some of the pertinent geometric characteristics of the two configurations are presented in table I.

SCOPE OF THE STUDY

The computation of aerodynamic stability derivatives was limited to low angles of attack (5.73° for the unswept-wing model and 4° for the swept-wing model) and low subsonic Mach number ($M \approx 0.16$). The derivatives computed were those listed in the section "Symbols" and are those generally considered to be important in aircraft dynamics. The procedures given in three well-known textbooks (refs. 1, 3, and 4), in an NACA Report (ref. 2), and in a U.S. Air Force sponsored publication (ref. 5) were followed in making the calculations. The experimental data used in conjunction with reference 2

were taken from reference 20. Results of the calculations are compared with wind-tunnel data and also with flight data for the D-558-II swept-wing configuration.

PRESENTATION OF RESULTS

The results of this study are presented in a series of charts which compare estimates of parameters as obtained from application of various published methods (refs. 1 to 5) and from wind-tunnel and flight data (refs. 20 to 26). All the data from wind-tunnel and flight test experiments are shown as solid symbols with those representing the flight test data being flagged. In some cases, estimated parameters are shown for various combinations of components to try to identify reasons why the analytical methods yield appreciably different results. The data are presented in the figures as shown in the following table:

Parameter	Figure
C_{L_α}	3
C_{m_α}	4
$d\epsilon/d\alpha$	5
C_{m_q}	6
$C_{m_{\dot{\alpha}}}$	7
$C_{m_q}+C_{m_{\dot{\alpha}}}$	8
C_{Y_β}	9
C_{n_β}	10
C_{l_β}	11
C_{Y_p}	12
C_{n_p}	13
C_{l_p}	14
C_{Y_r}	15
C_{n_r}	16
C_{l_r}	17

RESULTS AND DISCUSSION

The results are discussed in two separate sections: one related to longitudinal derivatives and the other to lateral derivatives. The wind-tunnel data are used as a basis for comparison of the results obtained by the various methods of estimating derivatives. The comparisons are first made for the complete airplane configuration. If the agreement between estimates and wind-tunnel results is poor, additional comparisons are made for various components of the configurations to try to identify the factors responsible for the differences.

Longitudinal Derivatives

C_{L_α} (fig. 3).- The estimated values of C_{L_α} were within 10 percent of the wind-tunnel results (refs. 21, 22, and 23). (See fig. 3.) The wing is the primary contributor to this parameter, and the differences in estimates obtained from the various references can be traced to differences in the wing contribution. These can, in turn, be associated with small differences in suggested values of section lift-curve slope, neglect of taper-ratio effects, or the form of the equation for C_{L_α}. It appears that all the methods used were about equally good for the two configurations of this study and that reference 5 was the best for the swept-wing configuration as is evident from a comparison of wind-tunnel data (refs. 22 and 23) and flight test data (ref. 24). It also appears from unpublished calculations that the smaller total C_{L_α} values obtained for the swept-wing configuration by using references 1 to 4 are due partly to neglect of or incorrect wing-fuselage effects.

C_{m_α} (fig. 4).- All except reference 4 of the analytical methods predicted a small stable (negative) value of C_{m_α} for the unswept-wing configuration. (See fig. 4(a).) The wind-tunnel value was a small positive value. However, the data source (ref. 21) indicated that the experimental value probably was in error because of geometric asymmetries and should have been neutrally stable $\left(C_{m_\alpha} = 0\right)$. The range of computed values of C_{m_α} was from about 0.07 to -0.13 (fig. 4(a)), which corresponds to a static-margin range of from about -0.02 to 0.03. This range is quite reasonable, and it appears that all the computational methods were equally good for the unswept-wing configuration.

The estimated values of C_{m_α} for the complete swept-wing configuration varied from -0.42 to -0.87. The wind-tunnel (ref. 23) and flight-extracted values (ref. 24) were about -0.65. Since there was such a large spread in the calculated values, additional curves are shown in figure 4(b) to isolate the causes of the differences. It can be seen that the primary causes of the differences are in the estimated values of the fuselage and horizontal-tail contributions to C_{m_α}. Additional factors which are not readily apparent in figure 4(b) but which also have some effect are differences in downwash (fig. 5) and

interference factors. The value estimated by use of reference 3 came closest to the wind-tunnel and flight-test values (fig. 4(b)).

C_{m_q} (fig. 6).- The primary contribution to C_{m_q} comes from the horizontal tail, and a small increment is produced by the wing. The analytical methods of references 1 to 5 are all approximately the same when nondimensionalized in the same manner and, therefore, yield comparable results. Differences which do occur are associated with suggested values of section lift-curve slope or neglecting taper-ratio effects in estimating the horizontal-tail lift-curve slope. Interference effects, however, are responsible for the poor agreement for the swept wing by using reference 5. (See fig. 6.) There were no experimental values available for comparison with the estimated values.

$C_{m_{\dot{\alpha}}}$ (fig. 7).- The primary contribution to $C_{m_{\dot{\alpha}}}$ comes from the horizontal tail also. Since all the analytical methods used herein were based on the same reference, they all yielded approximately the same result. (See fig. 7.) There were no experimental values available for comparison with estimated values.

$C_{m_q}+C_{m_{\dot{\alpha}}}$ (fig. 8).- The sum of the derivatives C_{m_q} and $C_{m_{\dot{\alpha}}}$ is the effective damping-in-pitch parameter. For this study the computed values of the component coefficients (from figs. 6 and 7) were simply added. The combination parameter can be obtained experimentally from the rate of damping of an oscillation about the Y body axis. There were no experimental data available for the unswept-wing configuration; however, there was a source of values for the swept-wing configuration. These data were for free-flight tests with a model at $M = 0.6$ (ref. 25). The results from the model tests are in good agreement with the computations. (See fig. 8.)

Lateral Derivatives

C_{Y_β} (fig. 9).- The calculated data show large differences in the values of C_{Y_β} as estimated by the methods of the various references. (See fig. 9.) The following factors account for the major differences in the values obtained by the various methods.

Reference 1: (a) No procedure is given to account for the end-plate effect of the fuselage on the vertical-tail effectiveness. (b) No procedure is given to account for the fuselage contribution to C_{Y_β}. (c) No procedure is given to account for the effect of the horizontal tail on the vertical tail (end-plate effect) if the horizontal tail is located somewhere other than at the base of the vertical tail.

Reference 3: No procedure is given to account for any fuselage contribution to C_{Y_β}.

Reference 4: (a) No method is given to estimate the end-plate effect of the blunt-tail fuselage on the aspect ratio of the vertical tail. (b) No procedure is given to estimate the

end-plate effect of the horizontal tail on the vertical tail for a position of the horizontal tail other than at the extremities of the vertical tail.

C_{n_β} (fig. 10).- There was a rather wide range in estimated values of C_{n_β} for both airplane configurations. (See fig. 10.) Most of the differences are associated with the estimated contribution of the vertical tail to C_{n_β}. The low value obtained from the use of reference 4 for the swept-wing configuration is caused primarily by not properly accounting for the effects of the fuselage and horizontal tail on the lift-curve slope of the vertical tail.

C_{l_β} (fig. 11).- The values of C_{l_β} estimated by use of references 3, 4, and 5 are much higher (more negative) than the wind-tunnel value (ref. 21) or the values estimated by use of references 1 and 2 for the unswept-wing configuration. The estimated tail contribution exceeds the wing contribution, and the differences in estimated tail contributions are primarily responsible for the differences in C_{l_β} of the various estimates.

The estimated values of C_{l_β} for the swept-wing configuration vary over a large range. The reasons for the differences in computed values in this case can be identified quite readily as follows.

Reference 1: It is perhaps unfair to include an estimate of C_{l_β} for the swept-wing configuration from reference 1. The difficulty lies in the fact that although reference 1 discusses the importance of wing sweep on C_{l_β}, it gives no procedure for estimating this important effect.

Reference 4: The estimated value of C_{l_β} for the swept-wing configuration is somewhat low, primarily because the end-plate effects of the body and horizontal tail on the vertical tail are neglected.

C_{Y_p} (fig. 12).- Although C_{Y_p} itself is not of much importance in determining the dynamics of an airplane, it is important for correcting the other rolling derivatives if the center of gravity is changed. The total estimated values of C_{Y_p} for the unswept-wing configuration are generally less positive than the experimental value (ref. 21). (See fig. 12.) Most of this difference is caused by the estimated contribution of the vertical tail. The computations indicate a small positive increment due to the vertical tail, whereas the experimental data indicate a rather large positive increment. The estimated C_{Y_p} values of the swept-wing configuration are in very good agreement with experimental data (ref. 22).

C_{n_p} (fig. 13).- The estimated values of C_{n_p} were in reasonably good agreement with the experimental values (refs. 21 and 22) for the unswept-wing and for the swept-wing configurations. (See fig. 13.)

C_{l_p} (fig. 14).- The primary contribution to C_{l_p} comes from the wing. Application of references 2, 3, 4, and 5 results in underestimating the unswept-wing contribution to C_{l_p}, and thereby also underestimating the total C_{l_p} of the unswept-wing configuration. (See fig. 14.) Extrapolation of the C_{l_p} curves given in reference 1 yields a value of C_{l_p} which is in good agreement with experimental data (refs. 21 and 22). All the methods yielded estimates of C_{l_p} for the swept-wing configuration which were very close to the experimental value (refs. 21, 22, and 24).

C_{Y_r} (fig. 15).- The parameter C_{Y_r} is generated almost totally by the vertical tail. References 1 and 4 did not present a specific method for computing C_{Y_r}; however, an estimate is readily obtainable from the C_{n_r} equations that are presented. There are no experimental data available for the unswept-wing configuration for comparison with the calculations. The computed results for the swept-wing configuration generally are greater than the experimental values (ref. 22), particularly the value estimated by using reference 5. (See fig. 15.) The large swept-wing value for reference 5 is primarly caused by $\left(1 + \frac{\partial\sigma}{\partial\beta}\right)\frac{q_V}{q_\infty}$ used in the $\left(C_{Y_\beta}\right)_V$ expression.

C_{n_r} (fig. 16).- The methods of references 1, 2, 3, and 5 yielded reasonably good estimates of C_{n_r} when compared with wind-tunnel data (refs. 22 and 26). (See fig. 16.) The omission of blunt-body end-plate effect on the vertical tail for reference 4 resulted in a large error for the tail contribution to C_{n_r} for the swept-wing configuration.

C_{l_r} (fig. 17).- Figure 17 shows that the estimated values of C_{l_r} were in fair agreement with each other for the unswept- and swept-wing configurations.

CONCLUDING REMARKS

Methods presented in five different publications have been used to estimate the low-speed aerodynamic derivatives of two unpowered airplane configurations. One configuration had unswept lifting surfaces, the other configuration was the D-558-II swept-wing research airplane. The results of the computations were compared with each other, with existing wind-tunnel data, and with flight-test data for the D-558-II configuration to assess the relative merits of the methods for estimating derivatives.

In general, it was found that all the methods gave reasonably accurate predictions for those derivatives which are attributed primarily to the wing and horizontal tail – mainly, the longitudinal derivatives. Even in these instances, however, there was some variation in the estimated horizontal tail and fuselage contribution to the pitching moments.

There were large differences between some of the lateral derivatives computed by using the various estimation methods. Most of the differences can be traced to the estimated vertical-tail effectiveness. A detailed comparison of tail-effectiveness estimates is not feasible because of differences in definitions of effective areas, span, interference effects, and so on.

The results of this study indicate that, in general, for low subsonic speeds, no one text appeared consistently better for estimating all derivatives.

Langley Research Center,
National Aeronautics and Space Administration,
Hampton, Va. October 14, 1971.

REFERENCES

1. Perkins, Courtland D.; and Hage, Robert E.: Airplane Performance Stability and Control. John Wiley & Sons, Inc., c.1949. (Reprinted 1957.)

2. Campbell, John P.; and McKinney, Marion O.: Summary of Methods for Calculating Dynamic Lateral Stability and Response and for Estimating Lateral Stability Derivatives. NACA Rep. 1098, 1952. (Supersedes NACA TN 2409.)

3. Etkin, Bernard: Dynamics of Flight – Stability and Control. John Wiley & Sons, Inc., c.1959.

4. Seckel, Edward: Stability and Control of Airplanes and Helicopters. Academic Press, Inc., c.1964.

5. Anon.: USAF Stability and Control Datcom. Contracts AF 33(616)-6460, AF 33(615)-1605, F33615-67-C-1156, F33615-68-C-1260, and F33615-70-C-1087, McDonnell Douglas Corp., Oct. 1960. (Revised Sept. 1970.)

6. Seckel, E.; and Morris, J. J.: The Stability Derivatives of the Navion Aircraft Estimated by Various Methods and Derived From Flight Test Data. Rep. No. FAA-RD-71-6, Jan. 1971. (Available from DDC as AD 723 779.)

7. Wolowicz, Chester H.; Strutz, Larry W.; Gilyard, Glenn B.; and Matheny, Neil W.: Preliminary Flight Evaluation of the Stability and Control Derivatives and Dynamic Characteristics of the Unaugmented XB-70-1 Airplane Including Comparisons With Predictions. NASA TN D-4578, 1968.

8. Burgin, George H.: Two New Methods for Obtaining Stability Derivatives From Flight Test Data. Contract No. NAS4-1280, Decision Sci., Inc., Sept. 1968. (Available as NASA CR-96005-Rev.)

9. Chevalier, Howard L.: Summary of Methods for Predicting the Dynamic Stability Characteristics of an Elastic Airplane. Transactions of the 3rd Technical Workshop on Dynamic Stability Problems, Vol. I, Paper 5, NASA Ames Res. Center, Nov. 1968. (Available as NASA TM X-62642.)

10. Thomas, H. H. B. M.: Estimation of Stability Derivatives (State of the Art). C.P. No. 664, Brit. A.R.C., 1963.

11. Lee, David G.: A Survey of Methods for Estimating the Damping-in-Pitch Parameter. Rep. 2816, Aero Rep. 1140, Naval Ship Res. Develop. Center, May 1968. (Available from DDC as AD 840 237.)

12. Members Aerodyn. & Struct. Res. Organ.: An Analysis of Methods for Predicting the Stability Characteristics of an Elastic Airplane. D6-20659-1 (Contract No. NAS 2-3662), Boeing Co., Nov. 1968. (Available as NASA CR-73277.)

13. Malthan, L. V.; and Hoak, D. E.: Current Progress in the Estimation of Stability Derivatives. AGARD Rep. 341, Apr. 1961.

14. Cole, Henry A., Jr.; Brown, Stuart C.; and Holleman, Euclid C.: Experimental and Predicted Longitudinal and Lateral-Directional Response Characteristics of a Large Flexible 35° Swept-Wing Airplane at an Altitude of 35,000 Feet. NACA Rep. 1330, 1957. (Supersedes NACA RM A54H09 by Cole, Brown, and Holleman, and TN 3874 by Brown and Holleman.)

15. Acum, W. E. A.: The Comparison of Theory and Experiment for Oscillating Wings. C.P. No. 681, Brit. A.R.C., 1963.

16. Rose, R.: Flight Measurements of the Dutch Roll Characteristics of a 60 Degree Delta Wing Aircraft (Fairey Delta 2) at Mach Numbers From 0.4 to 1.5 With Stability Derivatives Extracted by Vector Analysis. C.P. No. 653, Brit. A.R.C., 1963.

17. Fletcher, LeRoy S.: Dynamic Rotary Stability Derivatives of a Delta-Winged Configuration With a Canard Control and Nacelles at Mach Numbers From 0.25 to 3.50. NASA TM X-781, 1963.

18. Smutny, P.; and Wilson, M. C.: Wind Tunnel Investigation of Roll Rate Stability Derivatives – Exploratory Tests in BTWT With a Newly Developed Rotating Sting System. Doc. No. D6-20662-TN, Boeing Co., 1968. (Available from DDC as AD 671 676.)

19. Roskam, J.; and Dusto, A.: A Method for Predicting Longitudinal Stability Derivatives of Rigid and Elastic Airplanes. J. Aircraft, vol. 6, no. 6, Nov.-Dec. 1969, pp. 525-531.

20. Goodman, Alex: Effects of Wing Position and Horizontal-Tail Position on the Static Stability Characteristics of Models With Unswept and 45° Sweptback Surfaces With Some Reference to Mutual Interference. NACA TN 2504, 1951.

21. Letko, William; and Riley, Donald R.: Effect of an Unswept Wing on the Contribution of Unswept-Tail Configurations to the Low-Speed Static- and Rolling-Stability Derivatives of a Midwing Airplane Model. NACA TN 2175, 1950.

22. Queijo, M. J.; and Goodman, Alex: Calculations of the Dynamic Lateral Stability Characteristics of the Douglas D-558-II Airplane in High-Speed Flight for Various Wing Loadings and Altitudes. NACA RM L50H16a, 1950.

23. Queijo, M. J.; Jaquet, Byron M.; and Wolhart, Walter D.: Wind-Tunnel Investigation at Low Speed of the Effects of Chordwise Wing Fences and Horizontal-Tail Position on the Static Longitudinal Stability Characteristics of an Airplane Model With a 35° Sweptback Wing. NACA Rep. 1203, 1954. (Supersedes NACA RM L50K07 by Queijo and Jaquet and RM L51H17 by Queijo and Wolhart.)

24. Wolowicz, Chester H.; and Rediess, Herman A.: Effects of Jet Exhausts on Flight-Determined Longitudinal and Lateral Dynamic Stability Characteristics of the Douglas D-558-II Research Airplane. NACA RM H57G09, 1957.

25. Gillis, Clarence, L.; and Chapman, Rowe, Jr.: Summary of Pitch-Damping Derivatives of Complete Airplane and Missile Configurations as Measured in Flight at Transonic and Supersonic Speeds. NACA RM L52K20, 1953.

26. Fisher, Lewis R.; and Fletcher, Herman S.: Effect of Lag of Sidewash on the Vertical-Tail Contribution to Oscillatory Damping in Yaw of Airplane Models. NACA TN 3356, 1955.

TABLE I.- GEOMETRIC CHARACTERISTICS OF CONFIGURATIONS

[Center of gravity at quarter-chord of mean aerodynamic chord]

(a) Unswept-wing model

Wing:		
Aspect ratio	4.000	
Taper ratio	0.600	
Quarter-chord sweep angle, deg	0.000	
Incidence angle, deg	0.000	
Dihedral angle, deg	0.000	
Twist angle, deg	0.000	
Airfoil section	NACA 65A008	
Area, m^2 (ft^2)	0.209	(2.250)
Span, m (ft)	0.914	(3.000)
Mean aerodynamic chord, m (ft)	0.233	(0.765)
Vertical tail:		
Aspect ratio	2.000	
Taper ratio	0.600	
Quarter-chord sweep angle, deg	0.000	
Airfoil section	NACA 65A008	
Area, m^2 (ft^2)	0.031	(0.337)
Span, m (ft)	0.250	(0.821)
Mean aerodynamic chord, m (ft)	0.128	(0.419)
Longitudinal distance from center of gravity to vertical tail center of pressure, m (ft)	0.391	(1.282)
Vertical distance from center of gravity to vertical tail center of pressure, m (ft)	0.114	(0.376)
Horizontal tail:		
Aspect ratio	4.000	
Taper ratio	0.600	
Quarter-chord sweep angle, deg	0.000	
Incidence angle, deg	0.010	
Twist angle, deg	0.000	
Airfoil section	NACA 65A008	
Area, m^2 (ft^2)	0.0418	(0.450)
Span, m (ft)	0.409	(1.342)
Mean aerodynamic chord, m (ft)	0.104	(0.342)
Tail length, m (ft)	0.3907	(1.282)
Fuselage:		
Length, m (ft)	1.0158	(3.333)
Fineness ratio	6.670	

TABLE I.- GEOMETRIC CHARACTERISTICS OF CONFIGURATIONS – Concluded

[Center of gravity at quarter-chord of mean aerodynamic chord]

(b) Swept-wing (D-558-II) model

Wing:	
Aspect ratio	3.57
Taper ratio	0.57
30-percent-chord sweep angle, deg	35.00
Incidence angle, deg	3.00
Dihedral angle, deg	-3.00
Twist angle, deg	0.00
Airfoil section, root	NACA 63010
Airfoil section, tip	NACA 63012
Area, m^2 (ft^2)	16.258 (175.00)
Span, m (ft)	7.62 (25.00)
Mean aerodynamic chord, m (ft)	2.2159 (7.27)
Leading edge of $\bar{c}$ from leading edge of root chord, m (ft)	1.3746 (4.51)
Spanwise location of $\bar{c}$ from root chord, m (ft)	1.7068 (5.61)
Vertical tail:	
Aspect ratio	1.14
Effective aspect ratio	1.38
Taper ratio	0.18
30-percent-chord sweep angle, deg	49.00
Airfoil section, root	NACA 63010
Airfoil section, tip	NACA 63010
Area to body center line, m^2 (ft^2)	5.4626 (58.8)
Area of dorsal fin, m^2 (ft^2)	0.464 (5.0)
Span from fuselage center line, m (ft)	2.487 (8.16)
Mean aerodynamic chord (excluding dorsal fin), m (ft)	2.575 (8.45)
Tip chord (parallel to body center line), m (ft)	0.676 (2.22)
Root chord (parallel to body center line), m (ft)	3.758 (12.33)
Longitudinal distance from center of gravity to vertical tail center of pressure, m (ft)	5.124 (16.81)
Vertical distance from center of gravity to vertical tail center of pressure, m (ft)	1.0668 (3.5)
Horizontal tail:	
Aspect ratio	3.59
Taper ratio	0.50
30-percent-chord sweep angle, deg	40.00
Dihedral angle, deg	0.00
Airfoil section, root	NACA 63010
Airfoil section, tip	NACA 63010
Area, m^2 (ft^2)	3.7068 (39.90)
Span, m (ft)	3.642 (11.95)
Mean aerodynamic chord, m (ft)	1.0607 (3.48)
Height above fuselage center line, m (ft)	1.295 (4.25)
Tail length, m (ft)	5.916 (19.41)
Tip chord, m (ft)	0.6797 (2.23)
Fuselage:	
Length, m (ft)	12.8016 (42.00)
Fineness ratio	8.40

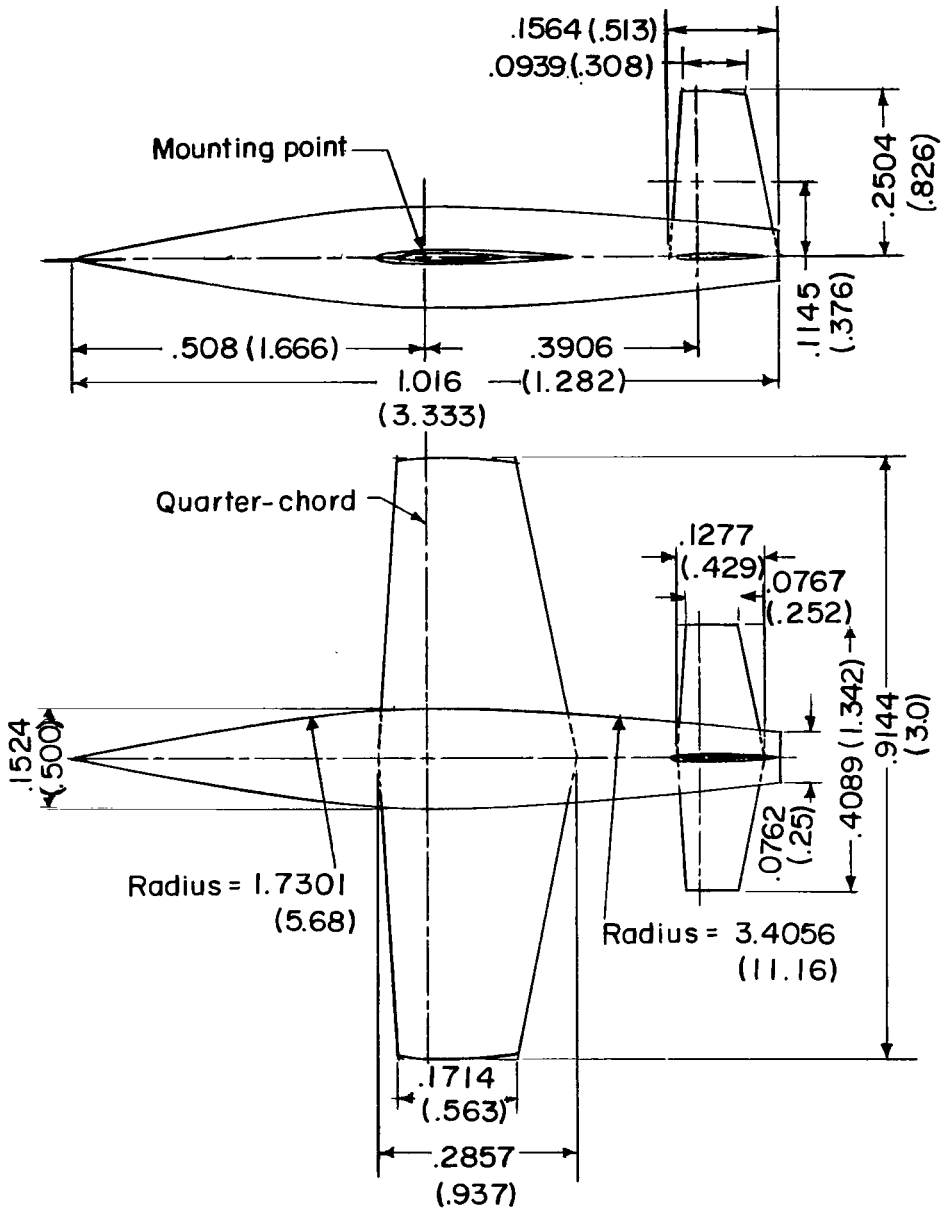

Figure 1.- Drawing of unswept-wing model. All dimensions are in meters (feet).

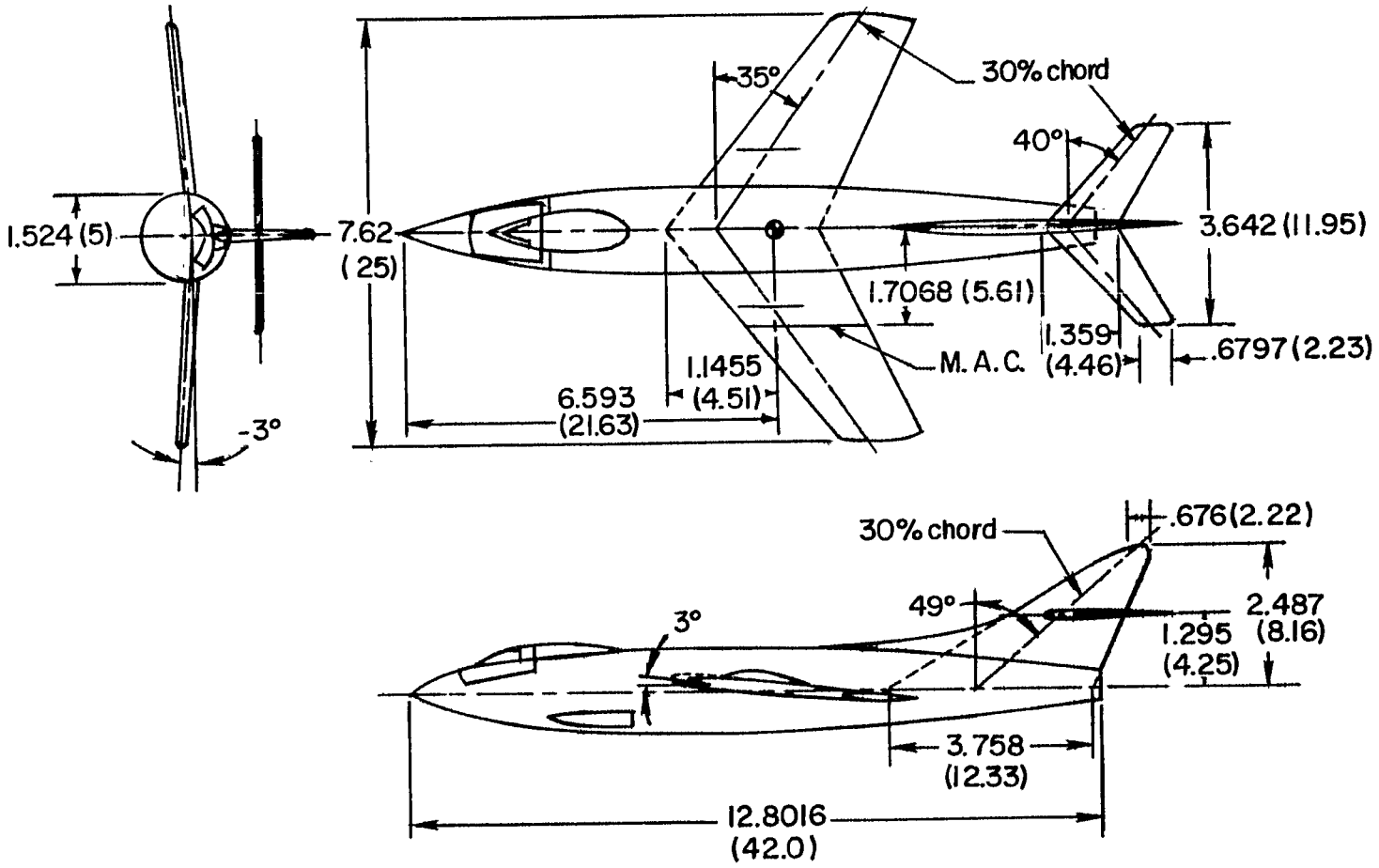

Figure 2.- Drawing of D-558-II swept-wing research airplane. All dimensions are in meters (feet).

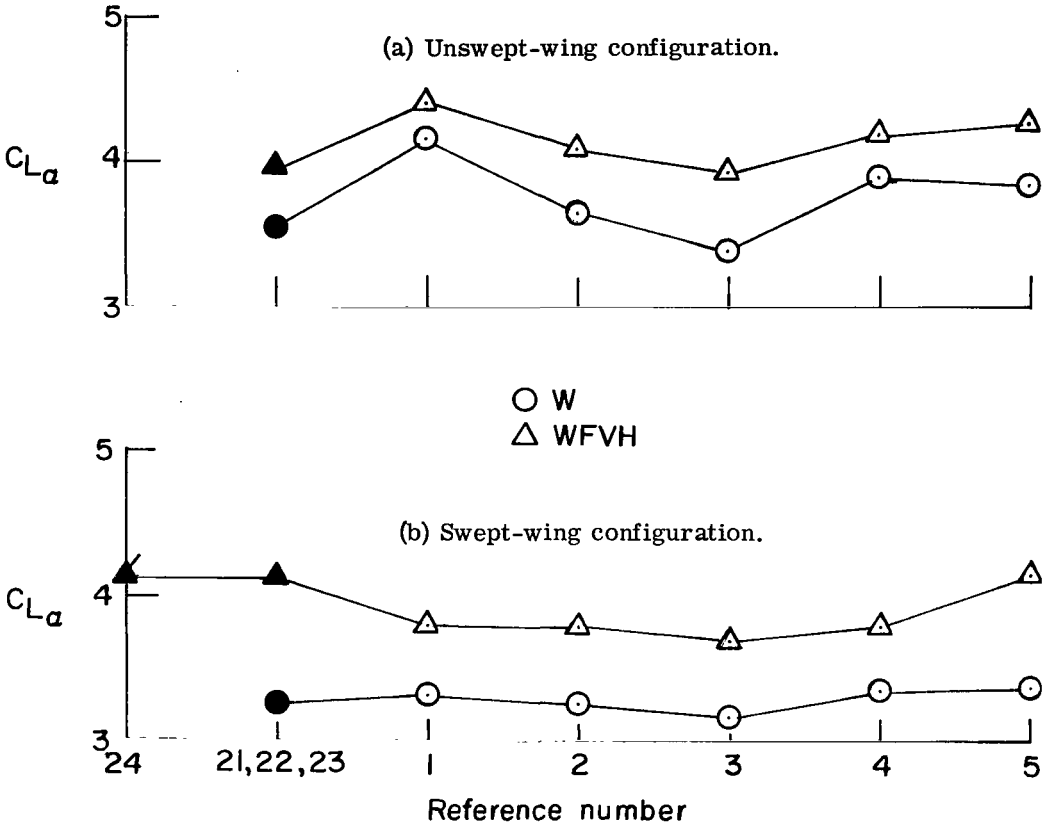

Figure 3.- Lift-curve slope. Solid symbols indicate experimental data; flagged symbol indicates flight test.

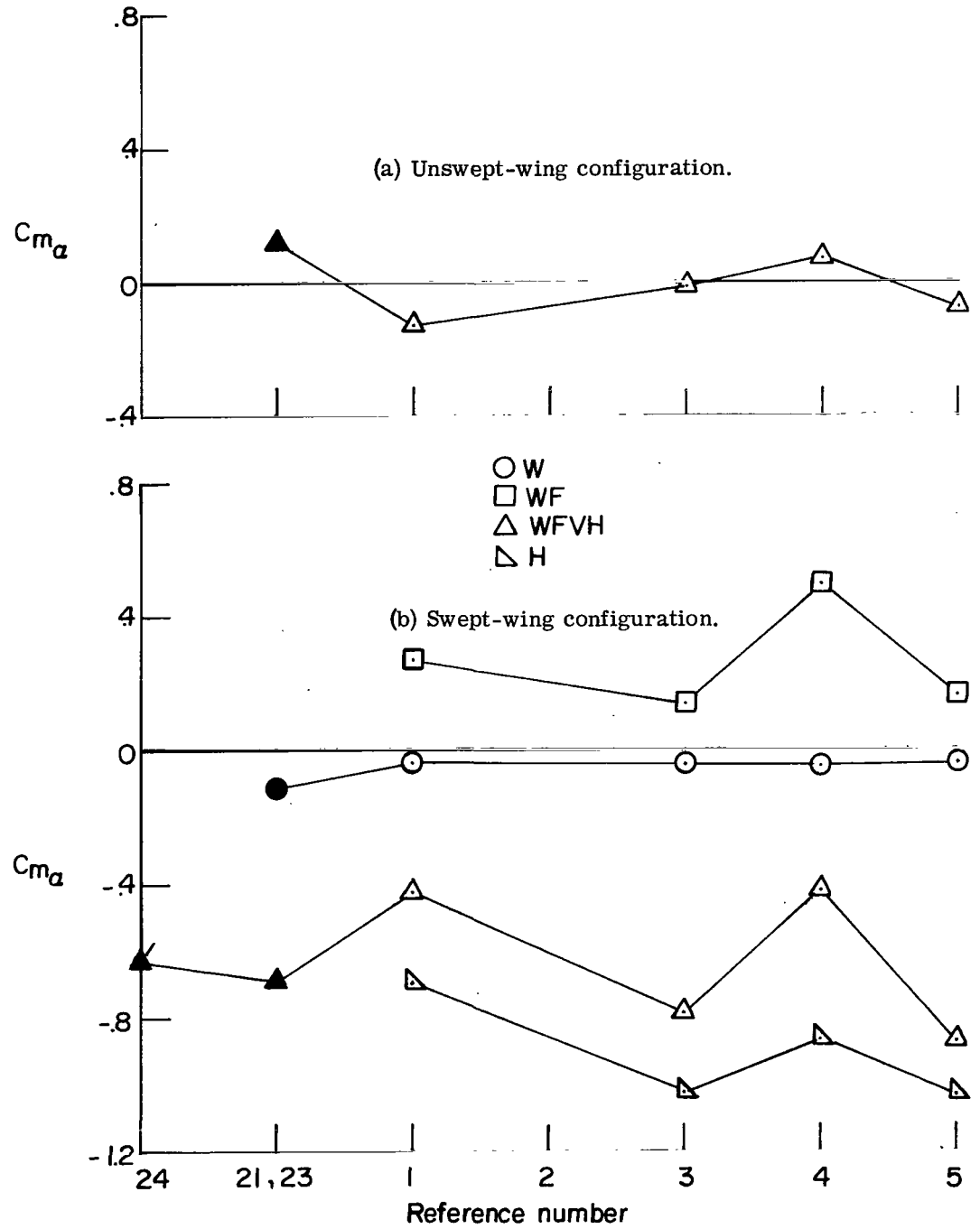

Figure 4.- Static longitudinal stability parameter. Solid symbols indicate experimental data; flagged symbol indicates flight test.

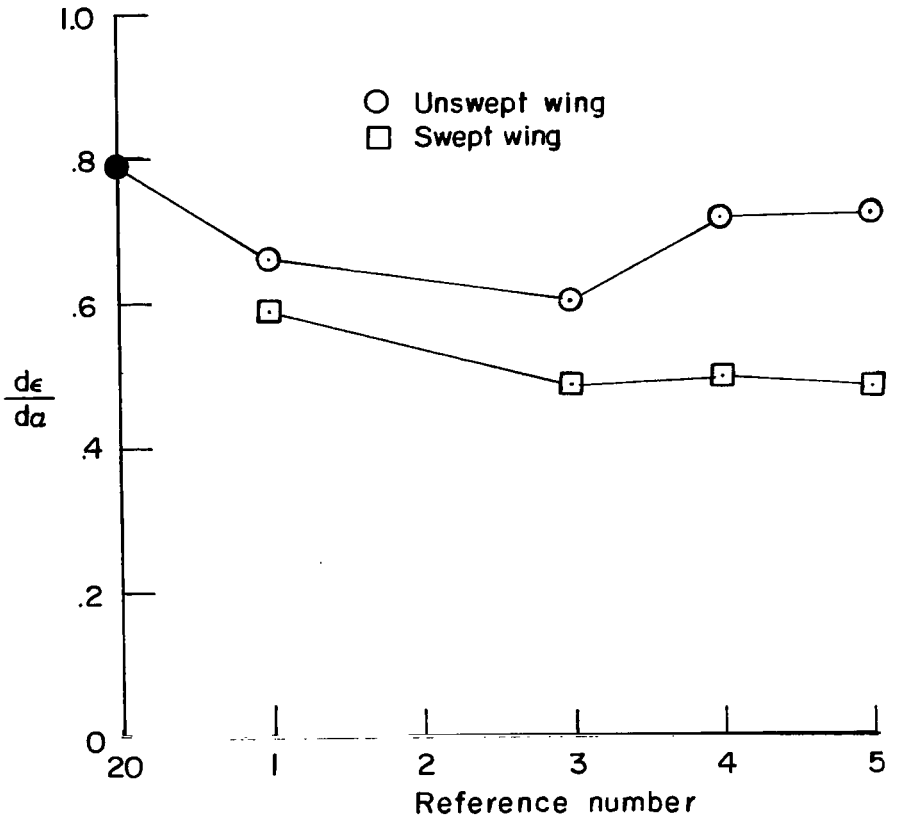

Figure 5.- Downwash parameter. Solid symbol indicates experimental data.

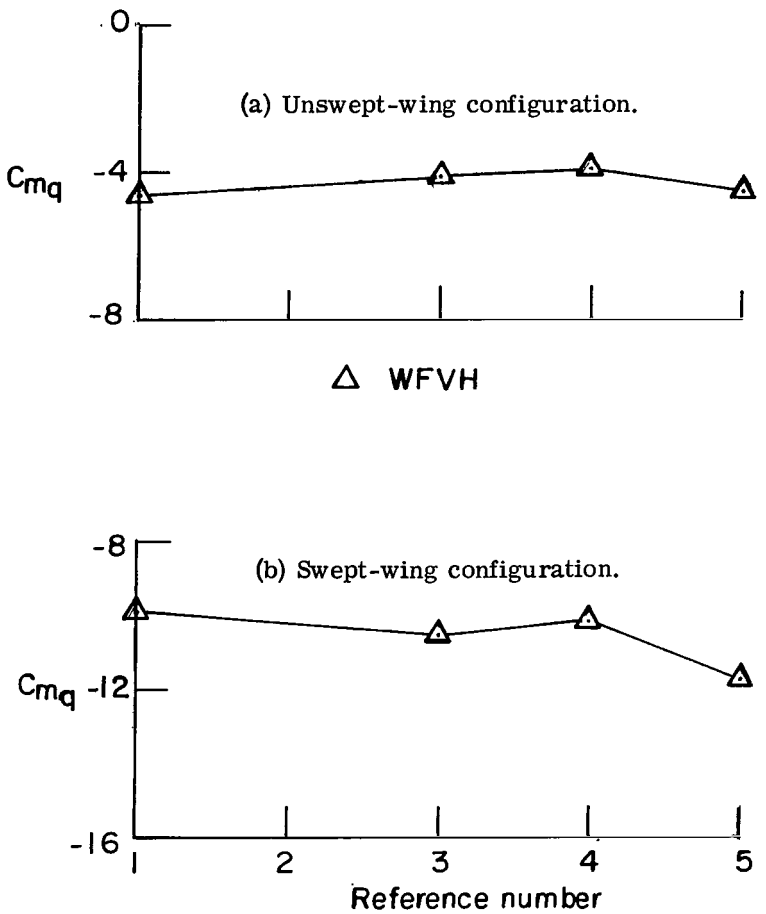

Figure 6.- Pitching moment due to pitching velocity or damping-in-pitch parameter.

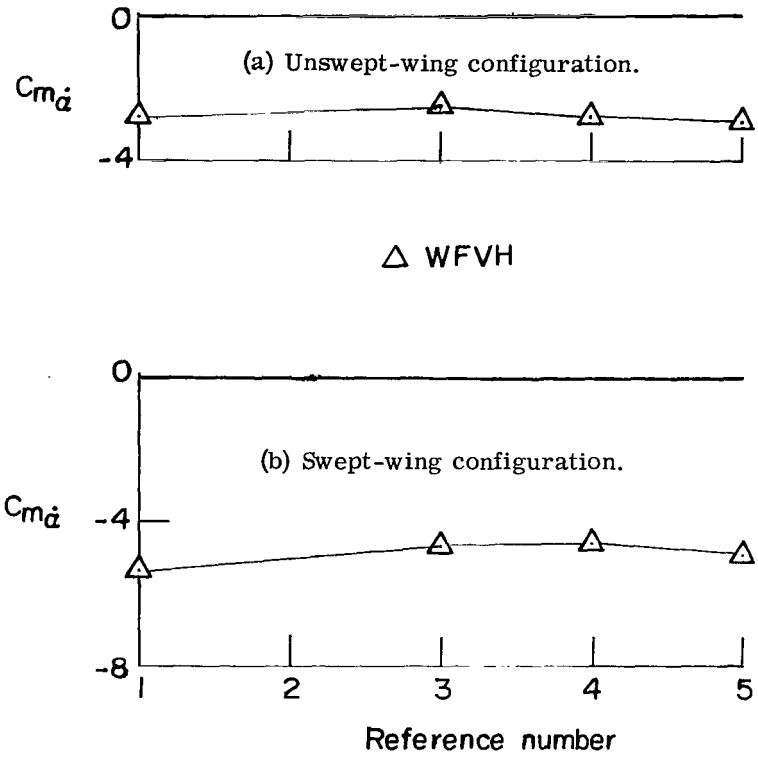

Figure 7.- Angle-of-attack damping parameter.

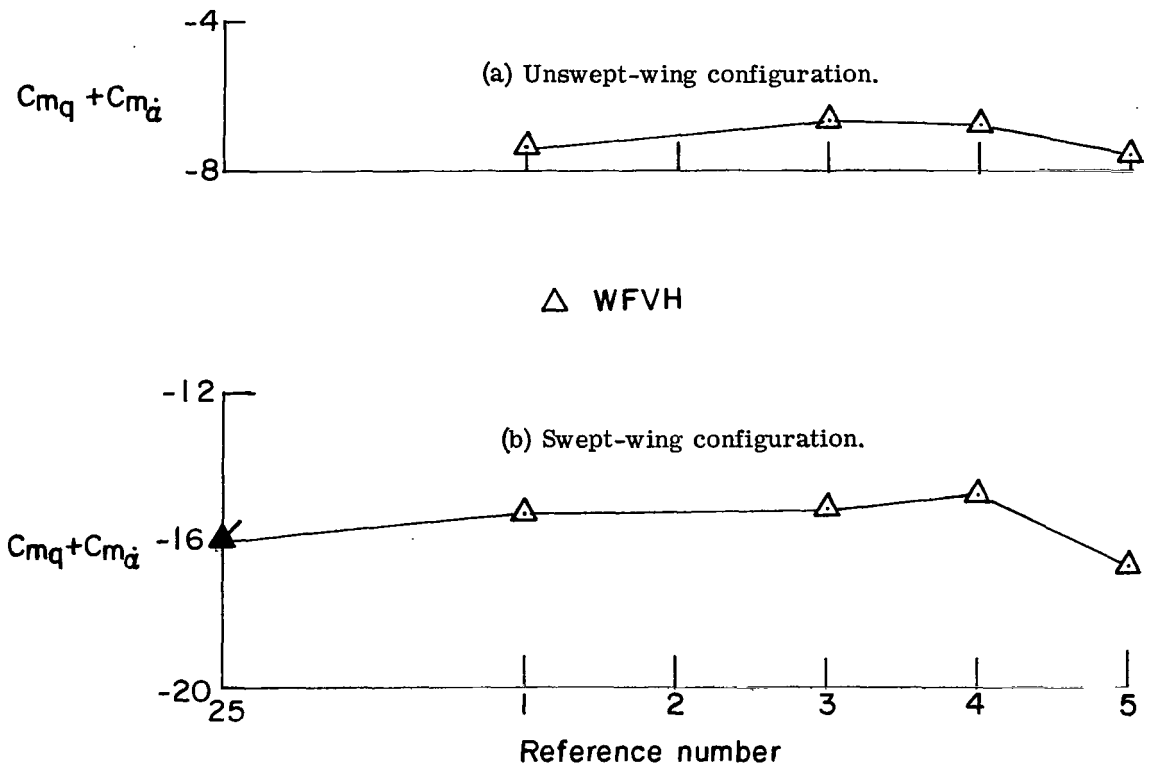

Figure 8.- Effective damping-in-pitch parameter. Solid flagged symbol indicates flight test data.

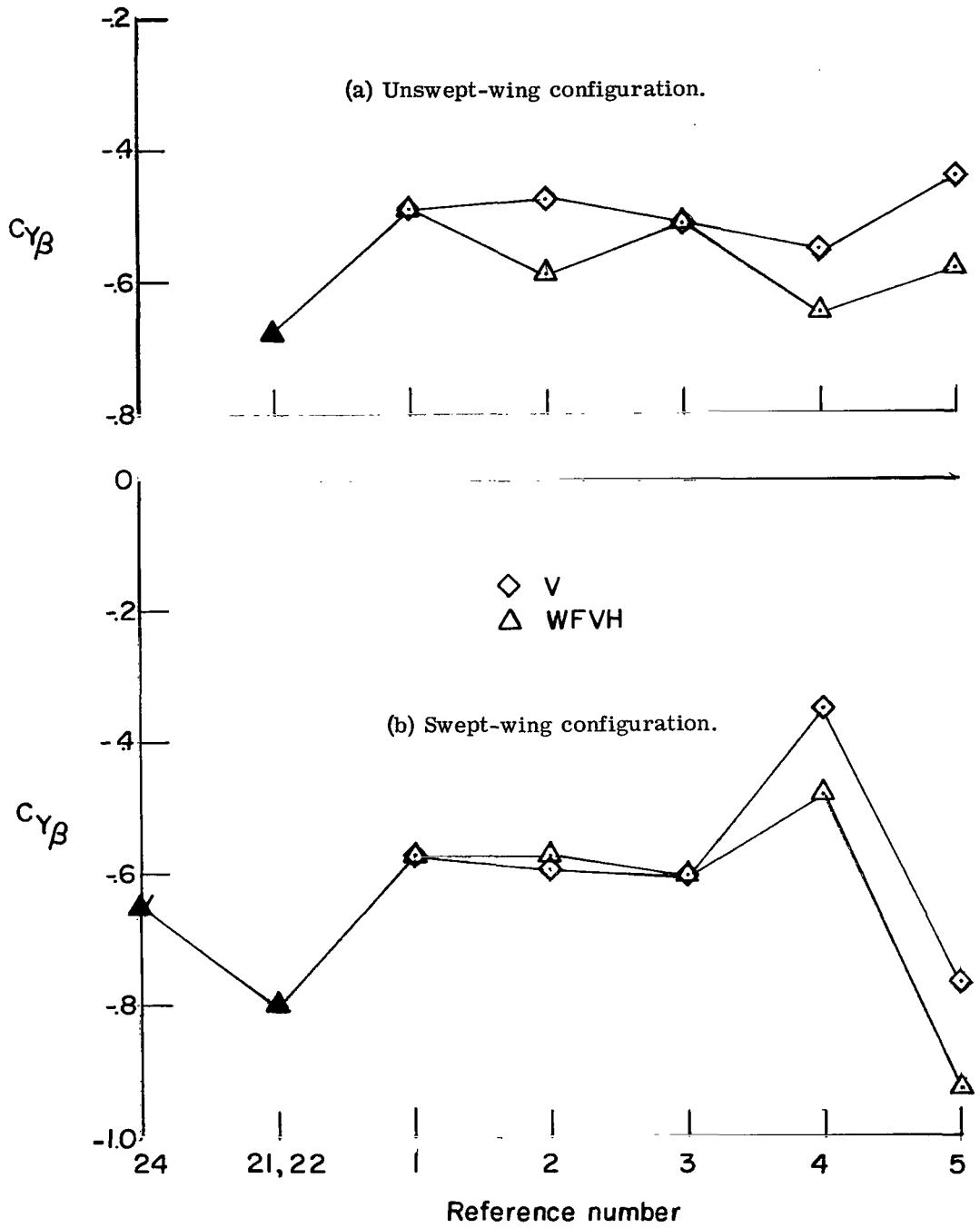

Figure 9.- Side force due to sideslip. Solid symbols indicate experimental data; flagged symbol indicates flight test.

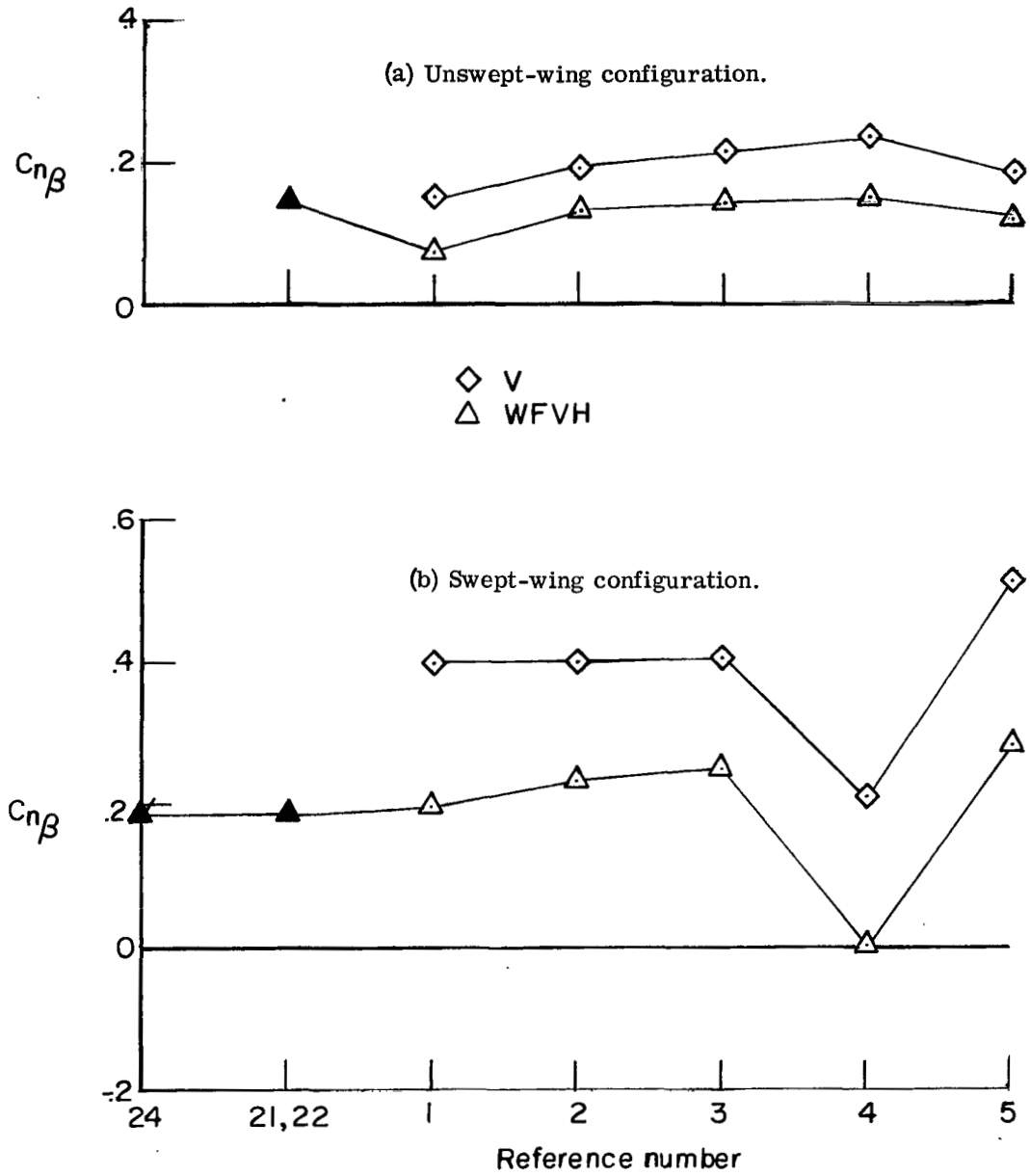

Figure 10.- Yawing moment due to sideslip. Solid symbols indicate experimental data; flagged symbol indicates flight test.

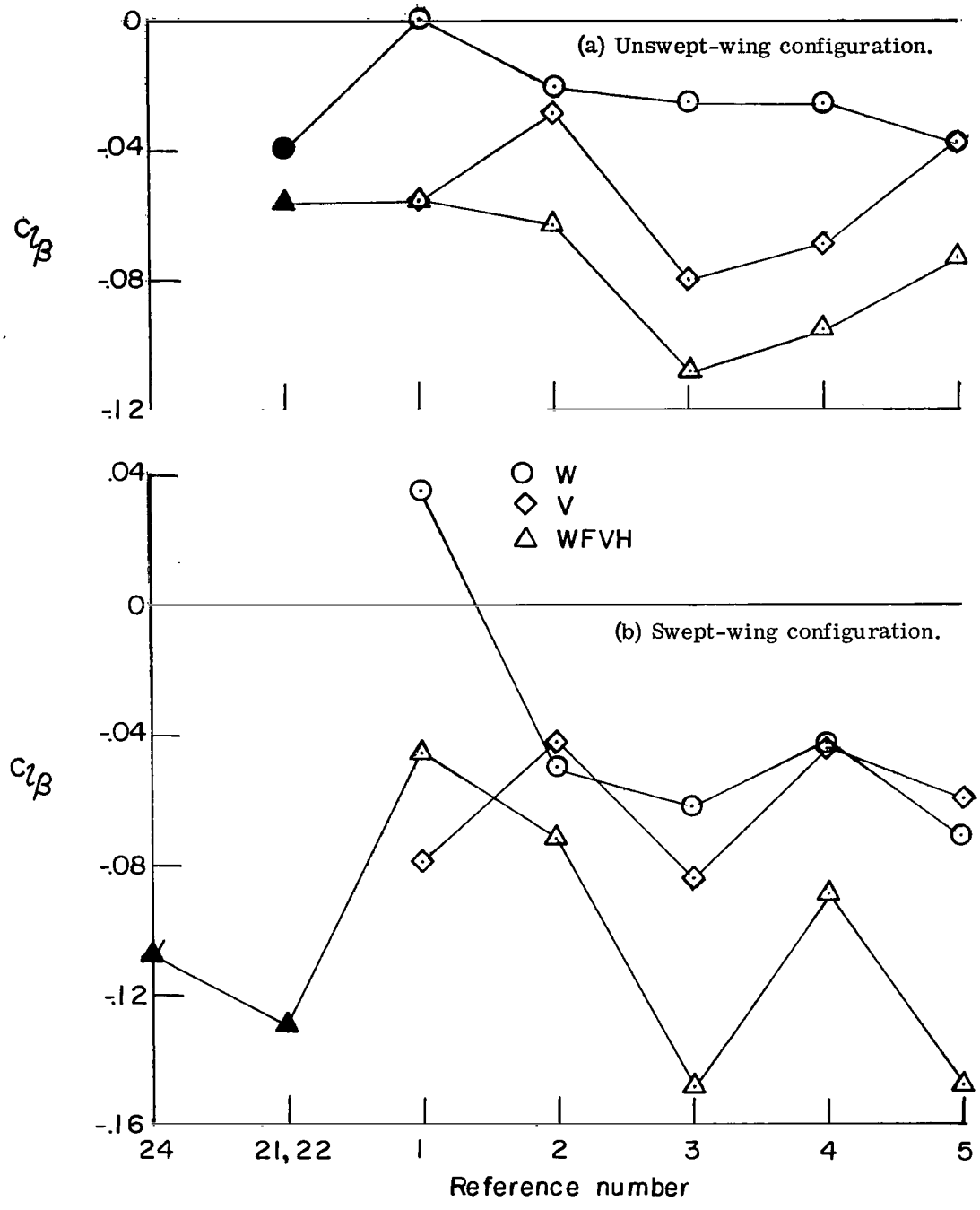

Figure 11.- Rolling moment due to sideslip or effective-dihedral parameter. Solid symbols indicate experimental data; flagged symbol indicates flight test.

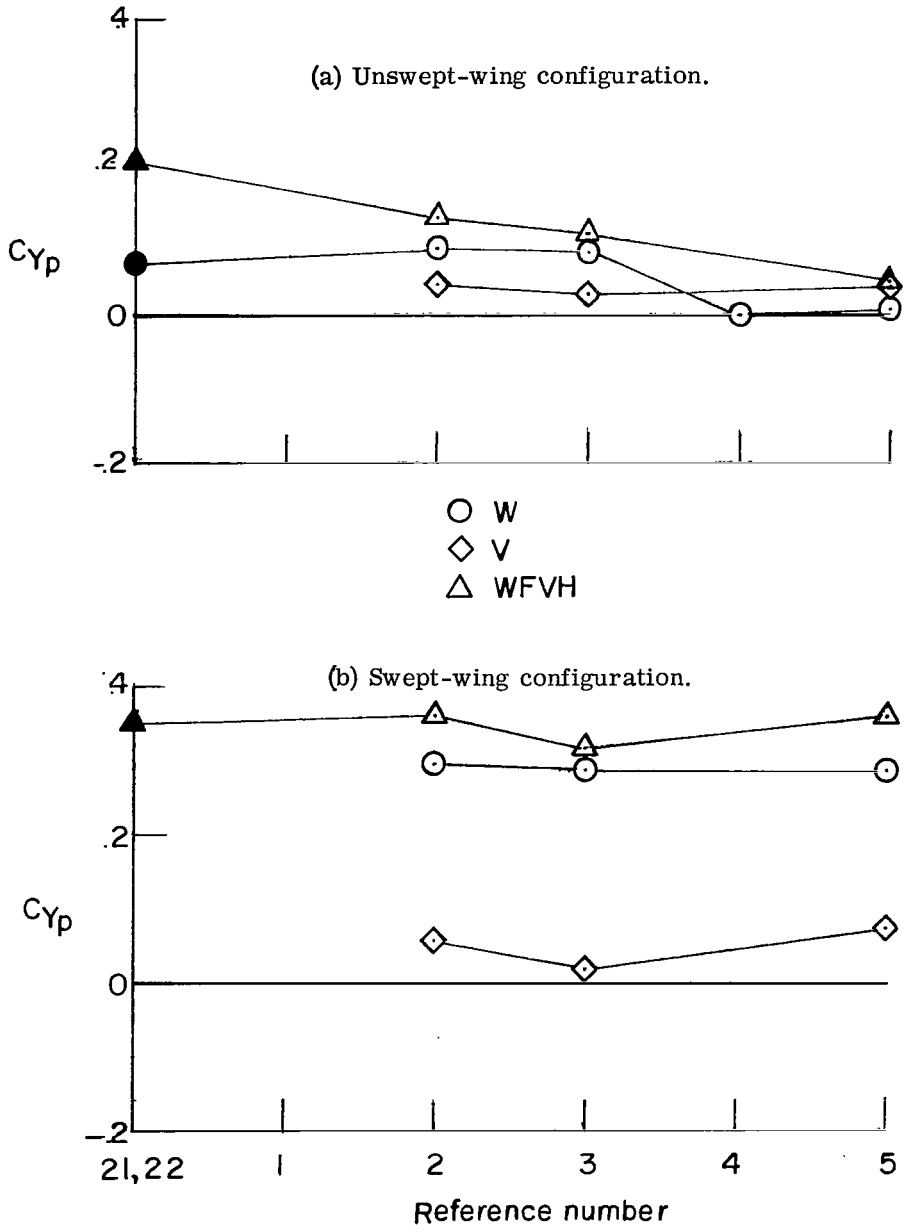

Figure 12.- Side force due to rolling velocity. Solid symbols indicate wind-tunnel data.

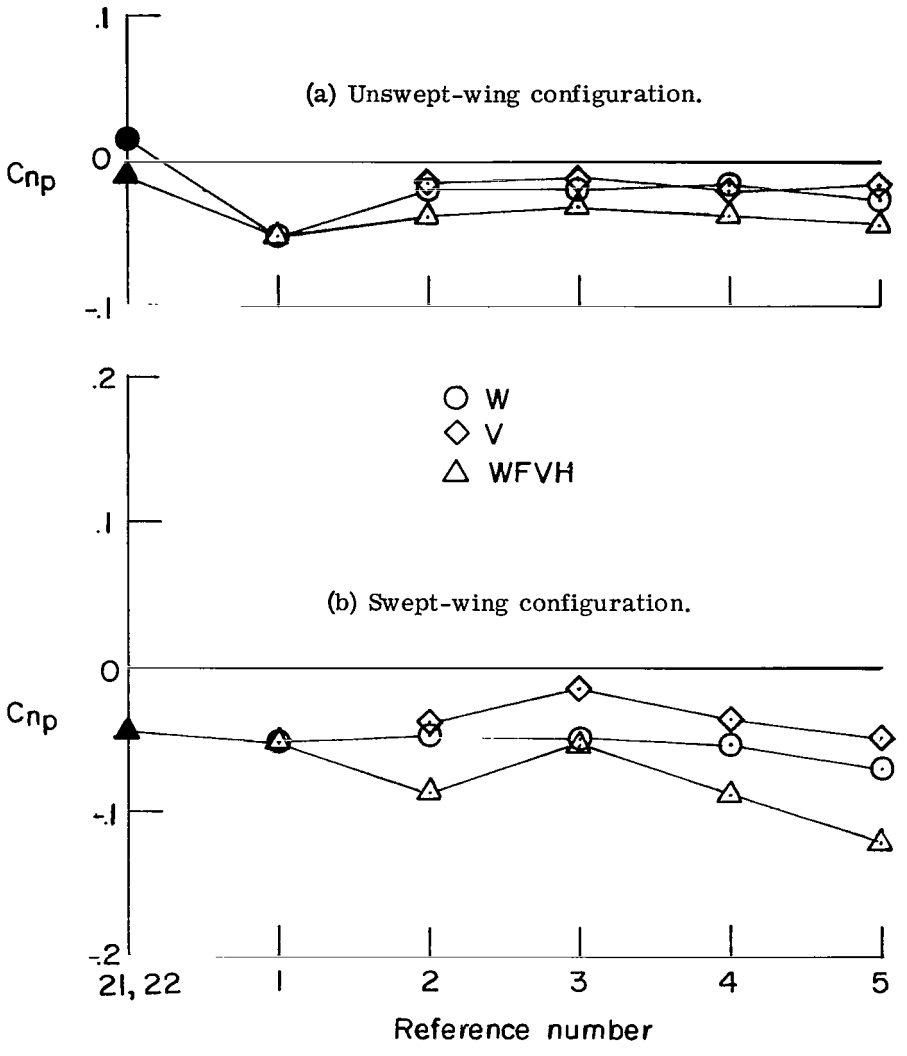

Figure 13.- Yawing moment due to rolling velocity or adverse-yaw parameter. Solid symbols indicate wind-tunnel data.

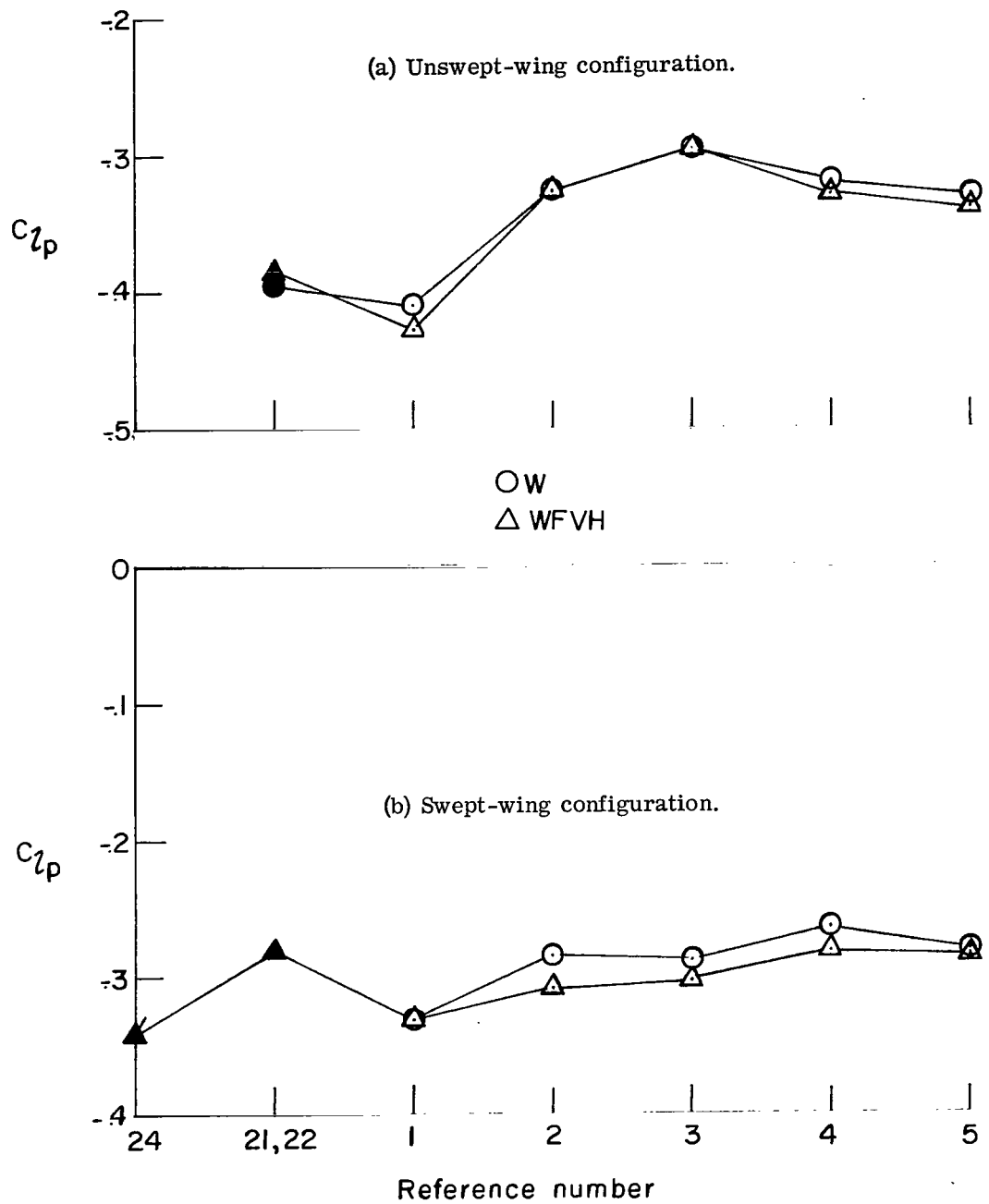

Figure 14.- Rolling moment due to rolling velocity or damping-in-roll parameter. Solid symbols indicate experimental data; flagged symbol indicates flight test.

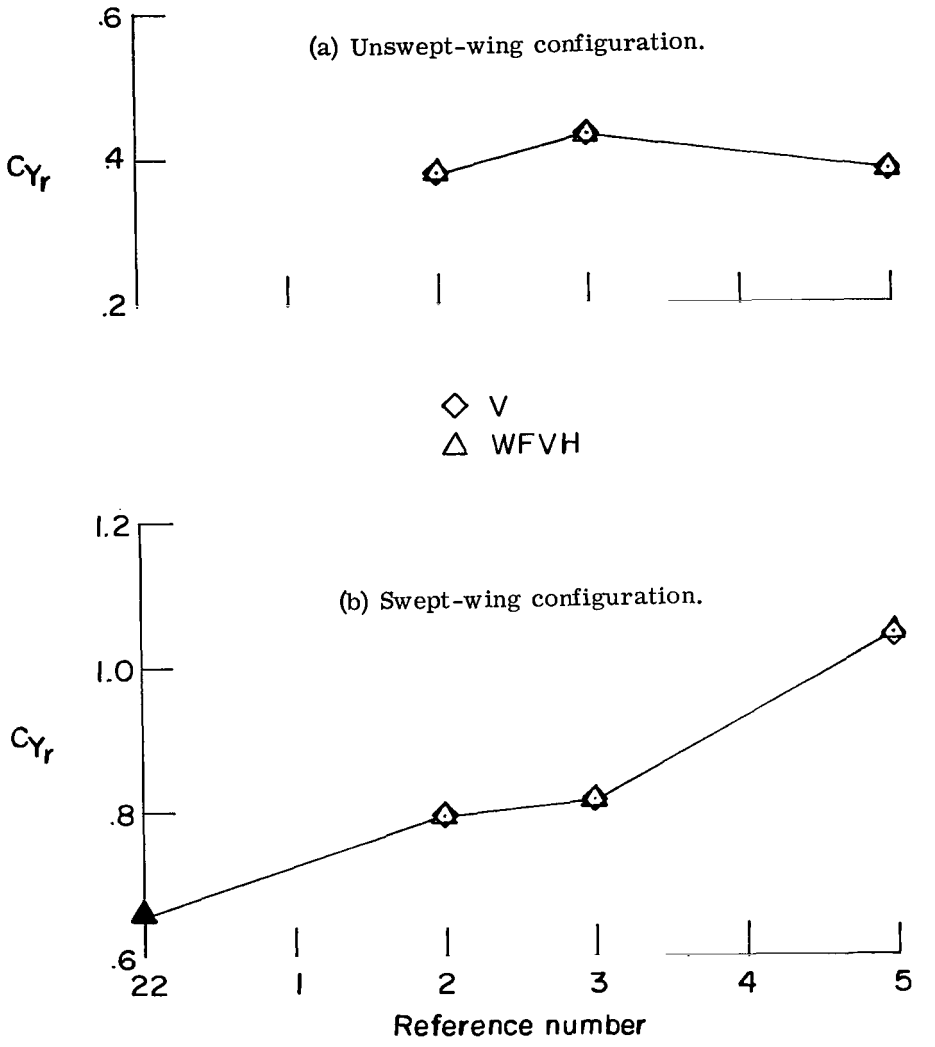

Figure 15.- Side force due to yawing velocity. Solid symbol indicates wind-tunnel data.

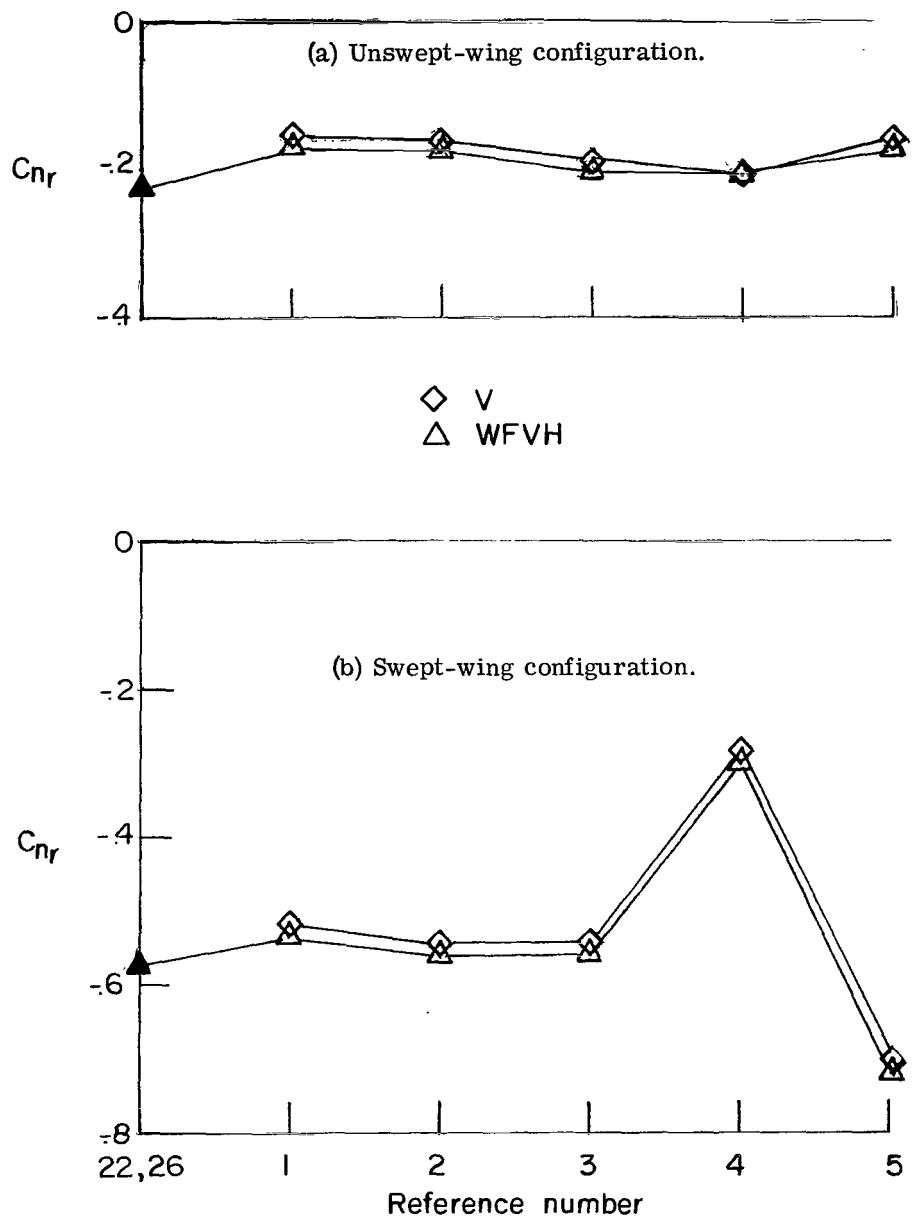

Figure 16.- Yawing moment due to yawing velocity or damping-in-yaw parameter. Solid symbol indicates wind-tunnel data.

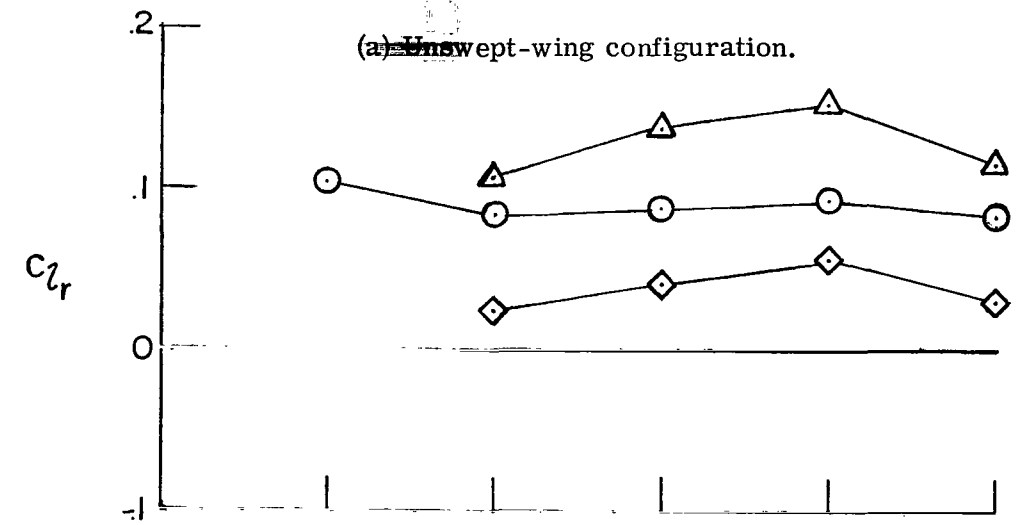

(a) Unswept-wing configuration.

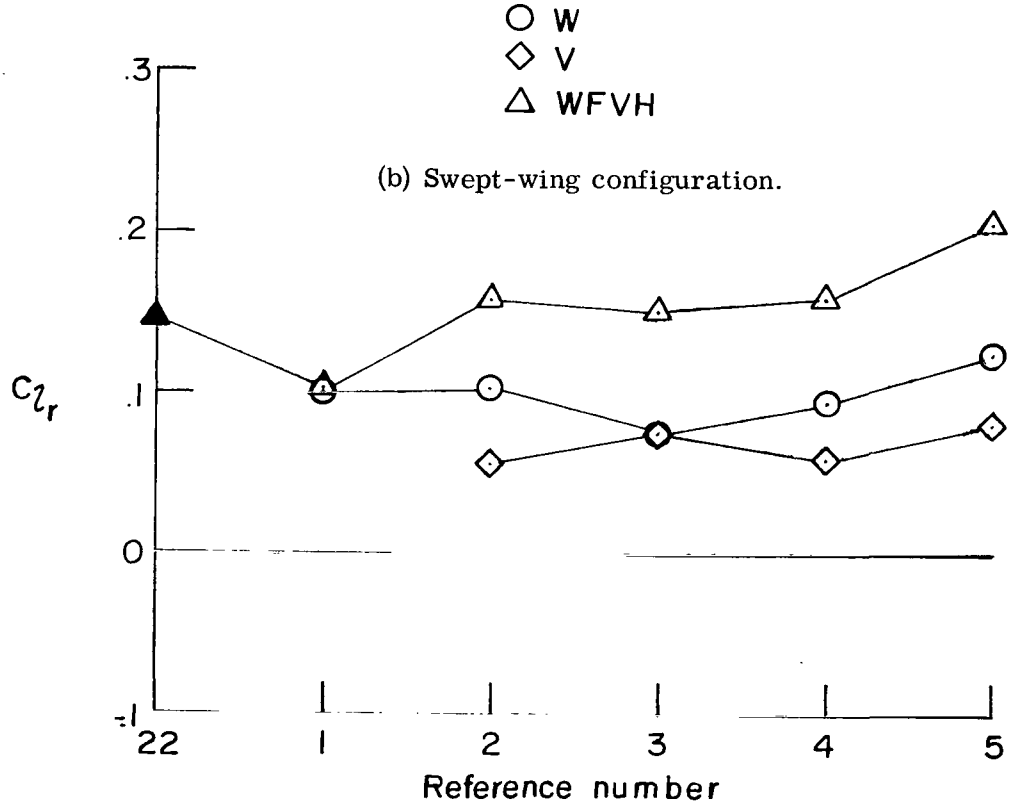

(b) Swept-wing configuration.

Figure 17.- Rolling moment due to yawing velocity. Solid symbol indicates wind-tunnel data.

"The aeronautical and space activities of the United States shall be conducted so as to contribute . . . to the expansion of human knowledge of phenomena in the atmosphere and space. The Administration shall provide for the widest practicable and appropriate dissemination of information concerning its activities and the results thereof."

— NATIONAL AERONAUTICS AND SPACE ACT OF 1958

NASA SCIENTIFIC AND TECHNICAL PUBLICATIONS

TECHNICAL REPORTS: Scientific and technical information considered important, complete, and a lasting contribution to existing knowledge.

TECHNICAL NOTES: Information less broad in scope but nevertheless of importance as a contribution to existing knowledge.

TECHNICAL MEMORANDUMS: Information receiving limited distribution because of preliminary data, security classification, or other reasons.

CONTRACTOR REPORTS: Scientific and technical information generated under a NASA contract or grant and considered an important contribution to existing knowledge.

TECHNICAL TRANSLATIONS: Information published in a foreign language considered to merit NASA distribution in English.

SPECIAL PUBLICATIONS: Information derived from or of value to NASA activities. Publications include conference proceedings, monographs, data compilations, handbooks, sourcebooks, and special bibliographies.

TECHNOLOGY UTILIZATION PUBLICATIONS: Information on technology used by NASA that may be of particular interest in commercial and other non-aerospace applications. Publications include Tech Briefs, Technology Utilization Reports and Technology Surveys.

Details on the availability of these publications may be obtained from:

SCIENTIFIC AND TECHNICAL INFORMATION OFFICE

NATIONAL AERONAUTICS AND SPACE ADMINISTRATION

Washington, D.C. 20546